ASTRO-H Hard X-ray Telescope (HXT)

Hisamitsu Awaki[a], Hideyo Kunieda[b], Akihiro Furuzawa[b], Yoshito Haba[b], Takayuki Hayashi[c], Ryo Iizuka[d], Kazunori Ishibashi[b], Manabu Ishida[c], Masayuki Itoh[e], Tatsuro Kosaka[f], Yoshitomo Maeda[c], Hironori Matsumoto[b], Takuya Miyazawa[b], Hideyuki Mori[c], Hosei Nagano[b], Yoshiharu Namba[g], Yasushi Ogasaka[h], Keiji Ogi[a], Takashi Okajima[i], Satoshi Sugita[a], Yoshio Suzuki[j], Keisuke Tamura[b], Yuzuru Tawara[b], Kentato Uesugi[j], Koujun Yamashita[h] and Shigeo Yamauchi[k]

[a]Ehime University, Bunkyo-cho, Matsuyama, Ehime 790-8577, Japan;
[b]Nagoya University, Furo-cho, Chikusa, Nagoya 464-8602, Japan;
[c]ISAS/JAXA, Yoshinodai, Chuou, Sagamihara 229-8510, Japan;
[d]Chuo University, Kasuga, Bunkyo, Tokyo 112-8551, Japan;
[e]Kobe University, Tsurukabuto, Nada, Kobe 657-8501, Japan;
[f]Kochi University of Technology, Tosayamada-cho, Kami, Kochi 782-8502, Japan;
[g]Chubu University, Matsumoto-cho, Kasugai, Aichi 487-8501, Japan;
[h]Japan Science and Technology Agency, 5-1 Gobancho, Chiyoda, Tokyo 102-0076, Japan;
[i]NASA's Goddard Space Flight Center, Greenbelt, MD 20771, USA;
[j]JASRI/SPring-8, Sayo-cho, Sayo, Hyogo 679-5198, Japan;
[k]Nara Women's University, Kitauoyanishi-machi, Nara, Nara 630-8506, Japan

ABSTRACT

The new Japanese X-ray Astronomy satellite, ASTRO-H will carry two identical hard X-ray telescopes (HXTs), which cover 5 to 80 keV, in order to provide new insights into frontier of X-ray astronomy. The HXT mirror surfaces are coated with Pt/C depth-graded multilayers to enhance hard X-ray effective area by means of Bragg reflection, and 213 mirror reflectors with a thickness of 0.22 mm are tightly nested confocally in a telescope. The production of FM HXT-1 and HXT-2 were completed in 2012 and 2013, respectively. The X-ray performance of HXTs were measured at the synchrotron radiation facility SPring-8/ BL20B2 Japan. The total effective area of two HXTs is about 350 cm^2 at 30 keV and the angular resolution of HXT is about 1.'9 in half power diameter at 30 keV. The HXTs are in the clean room at ISAS for waiting the final integration test.

Keywords: Hard X-rays, hard X-ray telescope, multilayer, depth-graded multilayer, ASTRO-H, HXT

1. INTRODUCTION

The new Japanese X-ray Astronomy satellite, ASTRO-H will be launched on HII-A, the Japan's primary large vehicle in 2015 [1]. ASTRO-H will carry four X-ray telescopes (XRTs), two soft X-ray imaging Telescopes (SXT) and two Hard X-ray imaging Telescopes (HXT) for the wide-band spectroscopy between 0.3 and 80 keV (see Figure 1). The hard X-ray imaging system is configured with Hard X-ray Imagers (HXI) which are the focal plane detectors of HXTs placed on the HXI plate of the extensible optical bench (EOB). The focal length of 12 m will be realized by extending the EOB.

The first full hard X-ray telescope was launched as a US-Japan international balloon experiment – InFOCμS – in 2001. In its maiden and two later flights, several X-ray sources (including Cyg X-1) were imaged in 20-40 keV to demonstrate its performance [2][3]. The hard X-ray reflectors onboard InFOCμS employed tightly-nested, conically-approximated thin-foil Wolter-I optics, and their reflector surfaces were coated with Pt/C depth-graded multilayers to enhance hard X-ray effective area by means of Bragg reflection [4]. The following balloon experiment SUMIT was performed in 2006 on the initiative of Nagoya University [5]. The success of the InFOCμS and SUMIT missions has been inherited by the ASTRO-H mission by JAXA.

*awaki@astro.phys.sci.ehime-u.ac.jp

Space Telescopes and Instrumentation 2014: Ultraviolet to Gamma Ray, edited by Tadayuki Takahashi, Jan-Willem A. den Herder, Mark Bautz, Proc. of SPIE Vol. 9144, 914426 · © 2014 SPIE
CCC code: 0277-786X/14/$18 · doi: 10.1117/12.2054633

ASTRO-H HXTs are designed to have total effective area of greater than 300 cm^2 at 30 keV and an angular resolution of 1.'7 (half power diameter), so that the hard X-ray imaging system of ASTRO-H will have a detection sensitivity 100 times higher than that of Suzaku [1] (Figure 2). ASTRO-H hard X-ray imaging system will provide new insights into frontier of X-ray astronomy.

In the next sections, design parameters of HXT are summarized together with those of the pre-collimators and thermal shields. In the third section, production of HXTs is shown, and the ground calibration is described in the section four.

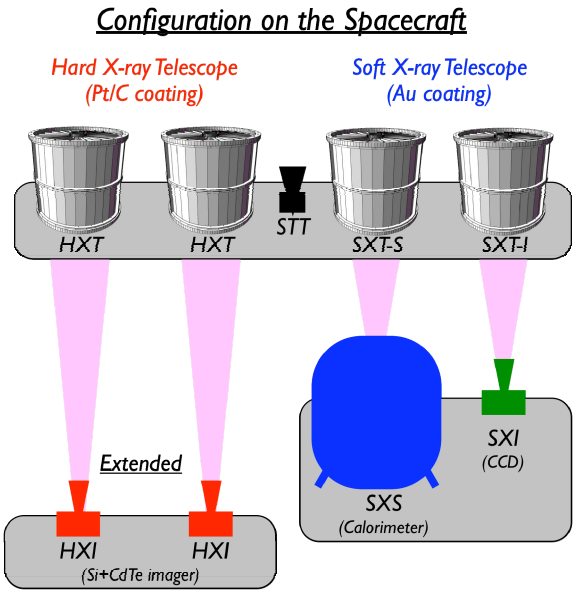

Figure 1 Configuration on the space craft

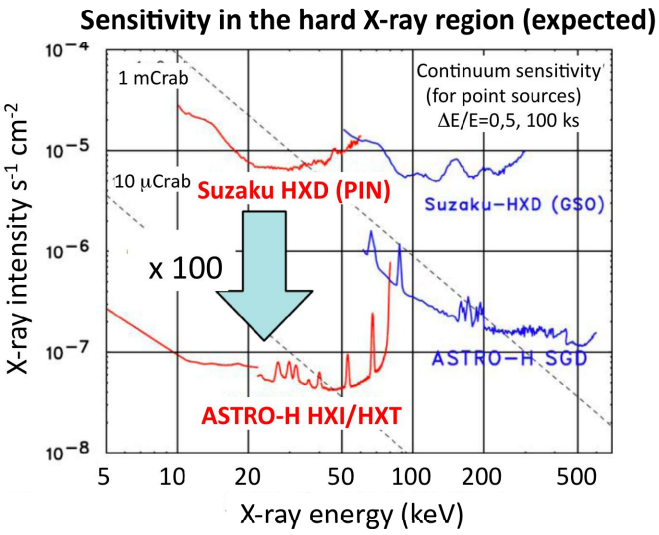

Figure 2 Sensitivity in the hard X-ray region, assuming the energy resolution ΔE/E=0.5 and the exposure time of 100 ks.

2. HARD X-RAY TELESCOPE

The HXT was designed based on the InFOCμS and SUMIT balloon-borne experiment [5][6] under the constraint on the space within the nose fairing of the HII-A rocket. Figure 3 shows a schematic view of the current design of HXT, and the design parameters of HXT are listed in Table 1. The basic design parameters of the HXT are 12 m focal length, 450 mm diameter, and 200 mm long foils. HXT consists of three components: two thermal shields (TS) [7], a pre-collimator (PC) [8], and reflector mirrors (primary and secondary mirrors). HXT has a reference cube, which is used to find the optical axis of a telescope with an accuracy of 5".

TS is used to cover the entrance side and bottom side of the telescope in order to reduce the radiative coupling between the HXT mirrors and the space/inside of the satellite [7][9]. TS is made of a polyethylene teleftalate (PET) film as thin as 2.5 μm, coated with an aluminum layer with a thickness of 30 nm, which has low solar absorptance and low infrared emissivity. Since the energy band of HXI covers 5 keV at the lower end, total thickness of PET equivalent thin film is determined to be 5 μm, in which the X-ray transmission of 5 μm PET is 98 %. In order to give enough mechanical strength to survive in various environments, a stainless steel mesh with a wire pitch, width, and thickness of 3 mm, 0.1 mm and 0.25 mm, respectively, is used to support the thin film. The transmission of soft X-rays down to 8 keV is 93 %.

PC (or stary-light baffle) consists of thin cylindrical shells, which are called blades. The Suzaku's PCs were mechanically independent from the mirror housing [10], but in the ASTRO-H HXT, the PC is integrated into the mirror housing, so that stray light is efficiently reduced without any loss of the on-axis effective area [11]. The height of the

blade measured from the top edge of the primary foil is determined to be 50 mm, in order to eliminate the secondary reflection from > 20’ off-axis from the HXI FOV (32 mm ×32 mm). Since the blade is installed in the top alignment bars (see Figure 3), there is a gap of 15 mm between the top edge of the mirror foil and the bottom edge of the blade. Thus the length of the blade is determined to be 35 mm.

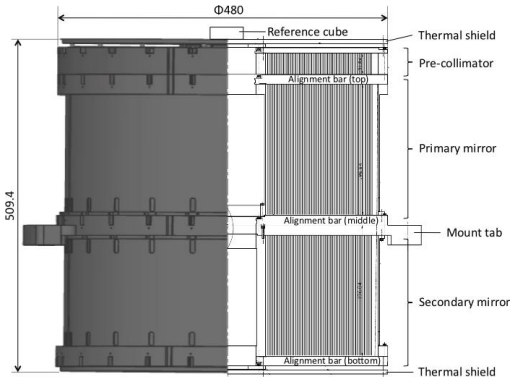

Figure 3 Schematic view of the HXT

Table 1 Design parameters of the HXT

Component	Item	HXT
Thermal shield	Thickness of aluminum coat	30 nm
	Film thickness	5 μm (PET)
	support	SUS mesh + Al frame + GFRP spacer
Pre-collimator	Blade height	50 mm
	Blade material	Aluminum, t0.15 mm
Mirror	Focal length	12 m
	reflector	t0.22 mm H200 mm 3 segmented
	Number of nest	213
	Number of reflector/telescope	1278
	Reflector surface	Pt/C multilayer

The blade thickness is 150 μm, which is thinner than that of the mirror substrate, and aluminum was selected as the blade material, because we had an experience of producing the PC blades made of aluminum for the Suzaku XRTs. Although a 150 μm thickness aluminum is transparent for photons above 50 keV, we confirmed that it does not affect the sensitivity of hard X-ray imaging system, since the X-ray background is very weak above 50 keV [8].

The HXT mirror employs conically-approximated thin-foil Wolter-I optics [6]. The approximated parabolic and hyperbolic foils are called primary and secondary reflectors in Figure 3, respectively. Image blurring due to the conical approximation is estimated to be about 0.’3 which is smaller than the requirement for the HXT. These reflectors are held at their desired location and confocally aligned by the grooves of alignment bars on each top and bottom edge of the reflectors. The diameters of the innermost and the outermost reflectors are 120 mm and 450 mm, respectively. To achieve high aperture efficiency despite the small incident angle, we use aluminum substrate with a thickness of 0.2 mm and a length of 200 mm. The reflector shells are confocally nested with maximal tightness. The total number of the nesting shells is determined to be 213. Since a shell is divided into 3 segments, 1278 reflectors are built into the telescope. The mirror surfaces are coated with Pt/C depth-graded multilayers to enhance hard X-ray effective area by means of Bragg reflection [12]. Figure 4 shows total effective areas with interfacial roughness of 0.3 nm, 0.4 nm, and 0.5 nm (Debye-Waller factor).

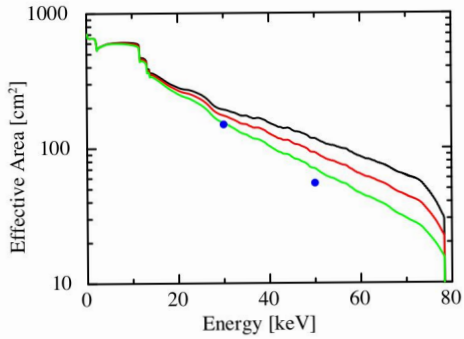

Figure 4 On-axis effective area of HXT (one telescope) with an interfacial roughness of 0.3 nm(black), 0.4 nm (red) and 0.5 nm (green). Assumed throughput is 0.75. Blue filled circles show the requirements.

3. PRODUCTION OF HARD X-RAY TELESCOPE

3.1 Production

Figure 5 shows a rough schedule of our HXT production. We started the design study of HXT in 2008. After the preliminary design review (PDR) of HXT in February 2010, we studied on the feasibility of the HXT design by simulations and tests with bread board model (BBM). Then, we finished the critical design review (CDR-1) of HXT in November 2011, and moved to fabrication stage of HXT flight model (FM).

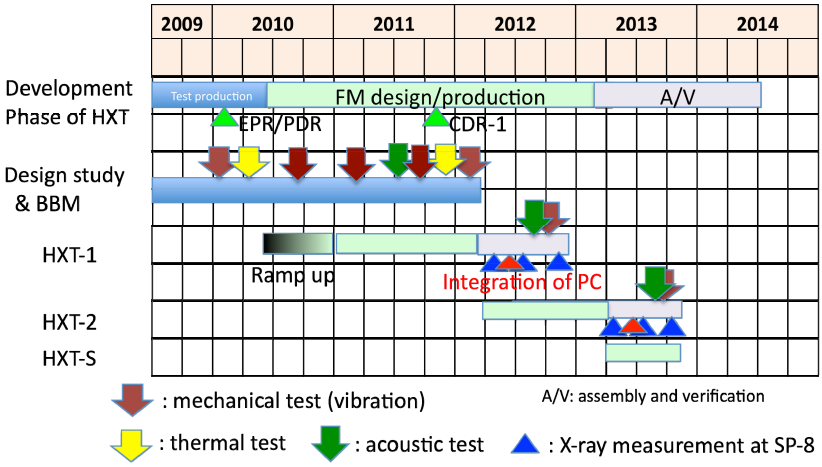

Figure 5 Rough schedule of HXT production

Since we estimated that we needed a few years for making a large number of reflector foiles, we started the mass-production of mirror foils in April 2010. Through a ramp-up phase in the early period of the mass production, we went ahead with production of the FM foils. The foil production for HXT-1 was completed in March 2012. We integrated the HXT-1, and then finished the integration in July 2012. We performed the acoustic and vibration tests, and confirmed that the X-ray properties were not changed before and after the tests. A year later, we completed the production of HXT-2.

3.2 Summary of Reflector Foil Production

The reflectors were fabricated by the epoxy-replication method in which a thin depth-graded Pt/C multilayer is sputtered onto the smooth surface of a glass tube and transferred to a conically shaped aluminum substrate with epoxy glue. In the large radius, we performed replication with GCM method, in which we used an aluminum mandrel wrapping a very thin flat glass around the mandrel surface as an glass tube. The procedure of the replication is described in Furuzawa et al. [13] . The production of HXT reflectors was carried out, using one spraying system and three sputtering chambers at Nagoya University [13]. During a production period of 3 years, 4576 foils have been made. This indicates that average production rate is 6 foils a day. We performed inspection to all productions, and 2982 foils among them were selected for FM and spare foils. The yield to make FM quality is about 65 %.

A mean surface roughness and a mean half power width of FM reflectors are measured to be 0.41 nm from X-ray reflection measurement and 0.’8 from optical measurements, respectively.

Table 2 summary of foil production

Production period	~ 3 years	
Total production	4576 foils	
Production rate	125 foils/month	= 6 /day
FM + Spare	2982 foils	Yield = 65 %
Glass mandrel	129	23 kinds of mandrel

3.3 Integration and Tuning

After the foil production, we performed the integration of HXT. The integration procedure is as follows,

1. Prepare the secondary housing and mirror reflectors.
2. Install thin foil mirrors into the secondary housing.
3. Tune the position of the middle alignment bars and the bottom alignment bars in SPring-8
4. Install thin foil reflectors into the primary housing

5. Tune the position of the top alignment bras in SPring-8

Tuning of the alignment bar position is essential to obtain a better imaging quality, because an X-ray image is distorted, if the bar positions are misaligned (see Figure 6). Tuning of the alignment bar positions was carried out at SPring-8 [14][15]. Figure 7 shows the HXT mounted on the telescope stage at the experimental hutch in SPring-8 BL20B2. There are 24 piezo motors, Piezo LEGS, connected to the alignment bars. The alignment bar can be moved in the radial direction, when the screws fasten the bars are loosed. We shifted the bar position by using the piezo motors with an accuracy of ~1 μm. Then, we obtained a round and compact X-ray image. The image location shift due to the corresponding alignment bar positioning error are 0.'15 in HXT1 and 0.'10 in HXT2. These are smaller than the requirement of HXT (1.'7).

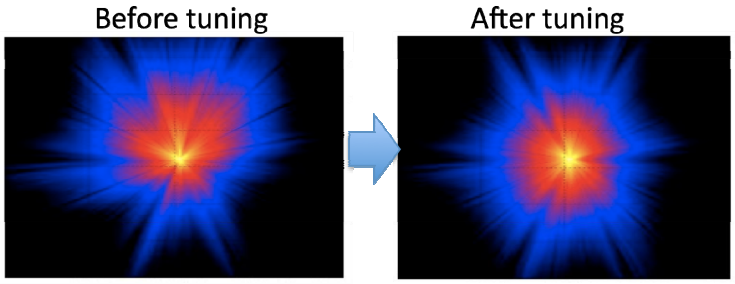

Figure 6 An example of improvement of X-ray image
Left and right images are before tuning and after tuning, respectively.

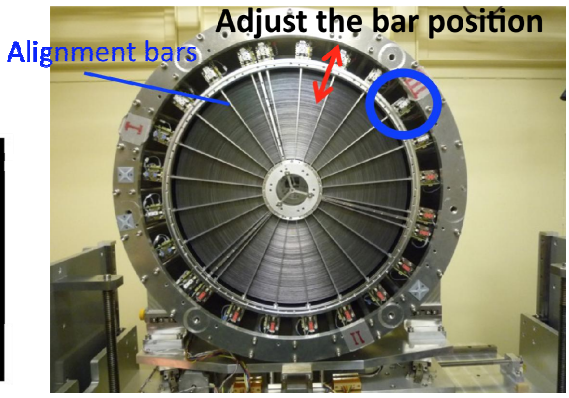

Figure 7 A picture during the adjustment of the bar positions. The blue circle shows a piezo motor connected to the HXT housing..

After installing PC blades, we completed the production of HXT. Figure 8 are pictures of HXT-1 and HXT-2. We note that X-ray properties and mechanical characteristics are quite similar. Thus, HXT-1 and HXT-2 are nearly identical. Now they are in the clean room at ISAS.

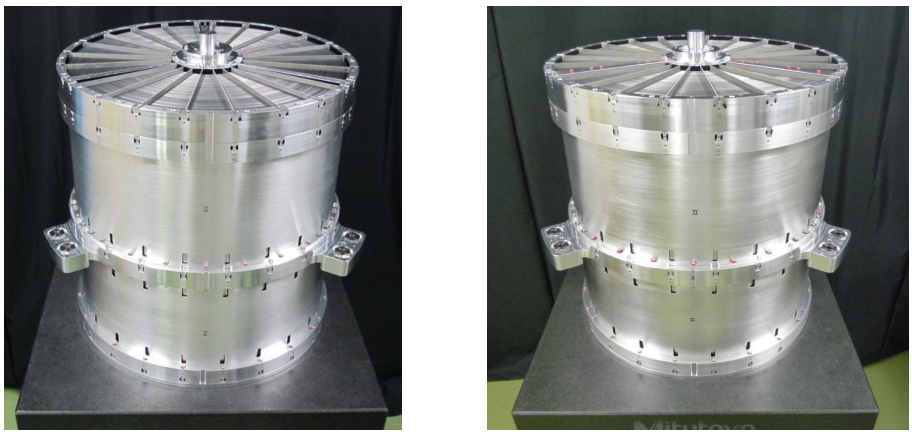

Figure 8 Pictures of HXT-1 (left) and HXT-2 (right)

4. GROUND CALIBRATION AT SPRING-8

4.1 Summary of the calibration items

We performed ground calibration at SPring-8. SPring-8 is one of the third-generation synchrotron radiation facilities in the world and is located in Hyogo, Japan. Since the total length of the beam line BL20B2 is 215 m [16], we can obtain a small beam divergence. In addition, the beam line has a double crystal monochromator (DCM) so that X-rays are monochromatized by the DCM. Thus, the beam line BL20B2 is suitable for the ground calibration of HXT. The properties of the BL20 B2 beam line are listed in Table 3.

Table 3 Characteristics of BL20B2

Energy Range	5-133 keV
E/ΔE	~10000
Beam divergence	2 arcsec / beam size (mm)

The calibration items are listed in Table 4. To obtain basic properties of HXTs, we measured both image quality and effective area at the several X-ray energies [15][17]. To find the optical axis of the telescopes, we measured the vignetting function of the telescopes. These data can be helpful to construct an off-axis image of the HXT. An HXT has a PC on the top of the telescope. Thus, we measured the reduction efficiency of the stray light due to the PC. Finally, we measured a detailed energy dependence of effective area with an energy step of 1 keV, since the energy response of the multilayer has structures due to Bragg-reflection. Details of the results of calibration are seen in Mori et al. 2014 [18].

Table 4 Calibration items in the ground calibration at SPring-8

Items / Energy (keV)	20	30	40	50	60	70
PSF/EEF + Effective area (E.A.)	2	1/2	1/2	1/2	1/2	1/2
Vignetting function		1		1/2		
Stray lights		1/2			2	
Detailed energy dependence of E.A.	2					

Note: 1: HXT1, 2: HXT2

4.2 X-ray characteristics

The beam line BL20B2 has the three experimental hutches located 44, 203 and 211 m from the light source, which are referred to as hutches 1, 2 and 3, respectively. By using both hutches 2 and 3, a 16 m-long experimental hutch is available for calibrations of HXTs, which have a long focal length 12m.

In our experiment at BL20B2, an HXT and an X-ray detector were set on motorized positioning stages in the hutches 2 and 3, respectively. Figure 9 is a schematic view of the measurement system at SPring-8 BL20B2.

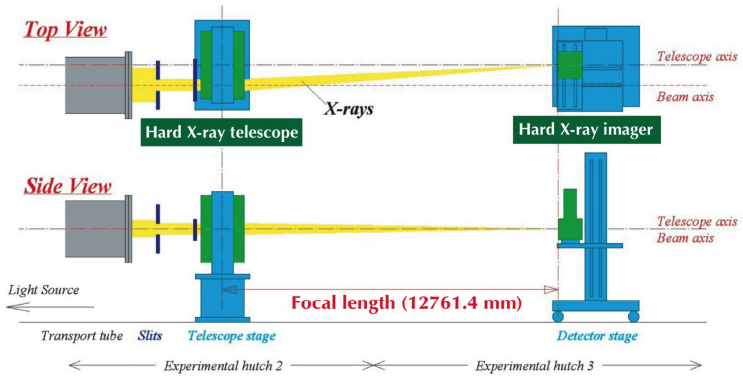

Figure 9 A schematic view of the measurement system [17]

The HXT was mounted on the telescope stage, and an X-ray imaging detector, which is an image intensifier (C7776) coupled to a CCD image sensor (C4480) made by HAMAMATSU Photonics K. K., was mounted on the detector stage. The plate scale and the number of the effective pixels of the detector are 19.3 μm/pixel and 4000 (H)×2624 (V), respectively. There was a four axis-slit in front of the telescope to shape the X-ray beam into 10×10 mm size. By scanning the full aperture of a segment with the 10×10mm X-ray beam (Figure 10), we obtained an X-ray image of the segment. By rotating the telescope stage, we derived the X-ray images of the other two segments. We constructed a full telescope image from these segment images.

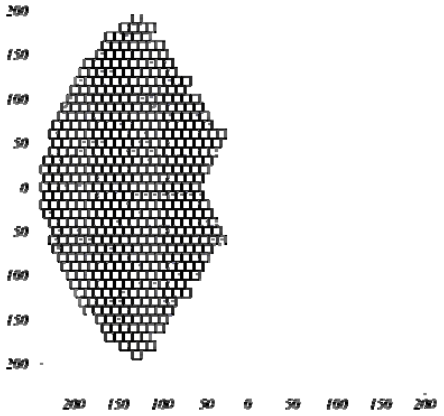

Figure 10 Scan path covering full aperture of one segment. Small squares present the size of the collimated X-ray beam with a 10 mm × 10 mm square. [18]

Figure 11 is an example of the full raster-scan image at 30 keV. A central 9.'2 × 9.'2 region is extracted from the original image. We made a radial dependence of the surface brightness, i.e., point spread function (PSF), and then produced an encircled energy function (EEF). In the HXT, the EEF is normalized at a radius of 6'. The half power diameter (HPD) is defined as the diameter at EEF=0.5. The HPD of HXT-2 at 30 keV is estimated to be 1.'88 (see Figure 12).

Effective area was calculated by accumulating photons within a radius of 4.'3. The effective area of HXT-2 at 30 keV was deduced to be 178 cm^2. Please note that these estimations of HPD and effective area are affected by stability of beam intensity, fluctuation of the background field, non uniformity of the imaging detector, and so on. In our estimation, the HPD has a systematic error of 0.'1 and effective area has a systematic error of about 1 % due to the ambiguity of the correction of them.

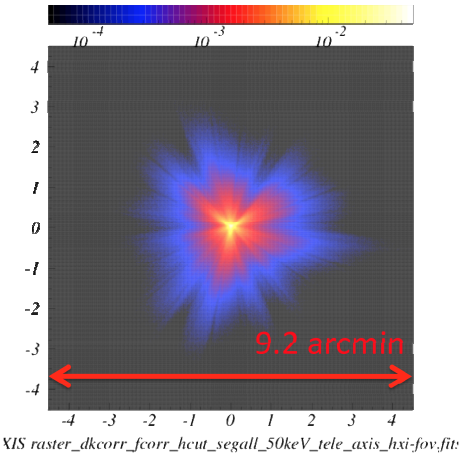

Figure 11 A full raster scan image of HXT-2 at 30 keV. The image size is 9.'2 square.

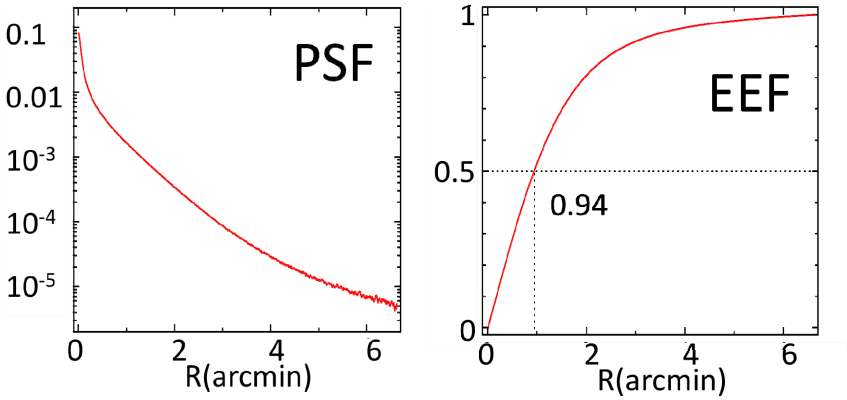

Figure 12 Point spread function (PSF) and encircled energy function (EEF) of the full scan image shown in Figure 11.

4.3 Summary of angular resolution and effective area

A summary of angular resolution of HXT-1 and HXT-2 is listed in Table 5. The angular resolutions of both HXT-1 and HXT-2 were measured to be about 1.'9 at 30 keV. There are no clear difference between HXT-1 and HXT-2, and the angular resolution has energy dependence. This energy dependence can be explained by the fact that the inner mirror shells have better image quality.

Table 6 is a summary of effective area. The effective areas of both HXT-1 and HXT-2 satisfy the requirements of 150 cm^2 at 30 keV, and 55 cm^2 at 50 keV. In the energy band below 50 keV, the effective area is well represented by a model with the roughness of the reflectors of 0.41 nm and with a throughput of 0.75. On the other hand, the measured effective area is smaller than that predicted by the model above 50 keV. We have not well understood the reason why there was a discrepancy between the measurement and the model. This might be caused by that we apply the Debye-Waller model in calculating the X-ray reflectivity.

Table 5 Angular resolution (HPD) measured at SPring-8

	20 keV	**30 keV**	**40 keV**	**50 keV**	**60 keV**	**70 keV**
HXT-1	---	1.92’	1.94’	1.80’	1.67’	1.49’
HXT-2	1.90’	1.88’	1.88’	1.78’	1.67’	1.55’

Note: these HPDs have a systematic error of 0.’1.

Table 6 Effective area measured at SPring-8

	20 keV	**30keV**	**40keV**	**50keV**	**60keV**	**70keV**
HXT-1	---	170 ± 2 cm^2	123 ± 1 cm^2	82 ± 2 cm^2	50 ± 1 cm^2	24.5 ± 0.4 cm^2
HXT-2	288 ± 3 cm^2	178 ± 1 cm^2	125 ± 1 cm^2	82 ± 0.4 cm^2	49.2 ± 0.3 cm^2	24.8 ± 0.4 cm^2

5. SUMMARY AND FUTURE PLAN

Development of HXT-1 and HXT-2 were started in 2008, and have been completed in 2013. We totally made 4576 foils during about 3 years, and selected 2982 foils for flight model or spare model. The properties of FM reflectors are as follows,

a mean surface roughness ~ 0.41 nm from X-ray reflection measurement
a mean half power width ~ 0.’8 from optical measurements.

Ground calibrations of HXTs at SPring-8 have been finished, and found that the X-ray properties of HXT-1 and HXT-2 are quite similar. The main results of the X-ray measurements are

HPD ~ 1.’9 at 30 keV and total effective area of HXT-1 and HXT-2 ~ 348 cm^2.

Since HXT has a large effective area below 10 keV, we will measure the effective areas at about 8 keV and 18 keV with the ISAS beam line [19]. The minimum dataset were almost obtained. Thus, we have a plan to make a calibration database.

The first integration test was performed at Tsukuba in May 2014 [20]. The integration test was successfully done. Figure 13 is a picture of the XRTs mounted on the top plate (see Figure 1).

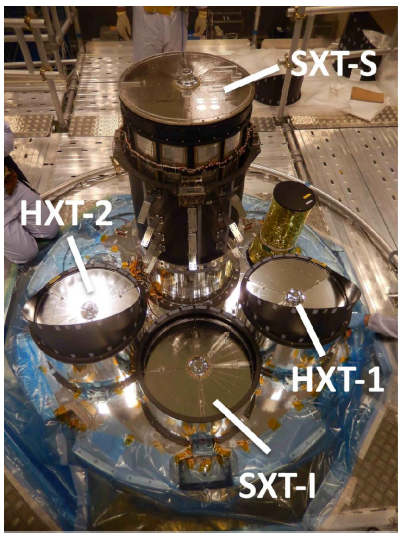

Figure 13 A picture of XRTs mounted on the top plate in the ASTRO-H first integration test.

The authors thank full time engineers and part time workers in Nagoya University for supports in the mass production of HXT mirror reflectors. The X-ray measurement was performed at BL20B2 in SPring-8, with the approval of the Japan Synchrotron Radiation Re- search Institute (JASRI).

REFERENCES

[1] Takahashi, T. et al. , "ASTRO-H mission", Proc. SPIE 7732, 77320Z (2010).

[2] Berendse, F. et al., "Production and Performance of the InFOCμS 20-40 keV Graded Multilayer Mirror", Applied Optics 42, 1856-1866 (2004).

[3] Ogasaka, Y. et al. , "First light of a hard-x-ray imaging experiment: the InFOCμS balloon ight", Proc. SPIE 5900, 217-224 (2005).

[4] Okajima, T. et al., "Characterization of the supermirror hard-x-ray telescope for the InFOCμS balloon experiment", Applied Optics 41, 5417-5426 (2002).

[5] Ogasaka, Y. et al. , "Thin-foil multilayer-supermirror hard x-ray telescopes for InFOCμS/SUMIT balloon experiments and NeXT satellite program", Proc. SPIE 6688, 668803 (2007).

[6] Kunieda, H. et al., "Hard x-ray telescope to be onboard ASTRO-H", Proc. SPIE 7732, 773214 (2010).

[7] Tawara, Y., Sugita, S., Furuzawa, A., Tachibana, K., Awaki, H., Ishida, M., Maeda, Y., and Ogawa, M. "Development of ultra-thin thermal shield for ASTRO-H x-ray telescopes", Proc. SPIE 7732, 77323A (2010).

[8] Mori, H. et al. "Current Status of the pre-collimator development for the ASTRO-H X-Ray Telescopes", Proc. SPIE 7732, 77323E (2010).

[9] Ito, K., Ogi, K., Awaki, H.,Koasaka, T., and Yamamoto, Y., "The thermal analysis of the Hard X-ray Telescope (HXT) and the investigation of the deformation of the mirror foil due to temperature change", Proc. SPIE 8147, 814704 (2011).

[10] Mori, H. et al., "Pre-Collimator of the Astro-E2 X-Ray Telescopes for Stray-Light Reduction", PASJ 57, 245-257 (2005).

[11] Mori, H. et al., "Design of the pre-collimator for the NeXT x-ray telescopes", Proc. SPIE 7011, 70112W (2008).

[12] Miyata, Y., Tamura, K., and Kunieda, H., "New multilayer design for ASTRO-H/hard x-ray telescope and missions beyond", Proc. SPIE 8147, 81470V (2011).

[13] Furuzawa, A., et al. , "The current status of ASTRO-H/HXT development facility", Proc. SPIE 7437, 743709 (2009).

[14] Awaki, H., et al., "Current status of ASTRO-H Hard X-ray Telescopes (HXTs)", Proc.SPIE 8443, 844324 (2012).

[15] Miyazawa, T., et al., “Recent results of hard X-ray characterization of ASTRO-H HXT at SPring-8”, Proc.SPIE 8443, 84435C (2012).

[16] Goto, S., et al., "Construction and commissioning of a 215-m-long beamline at SPring-8", Nucl. Instrum. Methods A, 467, 682-685 (2001).

[17] Miyazawa, T., et al., "Current status of hard x-ray characterization of ASTRO-H HXT at SPring-8", Proc. SPIE 7732, 77323 (2010).

[18] Mori, H., et al., “Recent progress in the ground calibration of the ASTRO-H Hard X-ray Telescope (HXT-2)”, Proc. SPIE 9144, in this proceedings (2014).

[19] Hayashi, T. et al., “Upgrade of the thirty-meter x-ray pencil beam line at the institute of space and astronautical science”, Proc. SPIE 9144, in this proceedings (2014).

[20] Takahashi, T., Mitsuda, K., and Kelly, R.L., “The ASTRO-H X-ray astronomy satellite”, Proc. SPIE 9144, in this proceedings (2014).